

Observation of Three-dimensional Long-range Order in Small Ion Coulomb Crystals in an rf Trap

A. Mortensen, E. Nielsen, T. Matthey, and M. Drewsen*

QUANTOP - Danish National Research Foundation Center for Quantum Optics,

Department of Physics and Astronomy, University of Aarhus, DK-8000 Aarhus C, Denmark

(Dated: May 24, 2019)

We present observations of three-dimensional long-range ordered structures in Coulomb crystals of $^{40}\text{Ca}^+$ ions confined in a linear rf Paul trap. In near-spherically symmetric crystals, we find an onset of body centered cubic structures in the crystal core when the number of ions exceeds ~ 1000 ions, a much smaller number of ions expected to be needed from ground state molecular dynamics (MD) simulations. Previously, three-dimensional long-range structures have only been observed and studied in Penning traps in systems of $\sim 100,000$ ions or more.

PACS numbers: 32.80.Pj, 52.27.Jt, 52.27.Gr, 36.40.Ei

A Coulomb crystal is the solid state phase of a confined ensemble of Coulomb interacting particles with the same sign of charge, often referred to as a one-component plasma (OCP). Coulomb crystallization and properties of Coulomb crystals have been studied for decades both theoretically and experimentally in such a variety of systems as 2D electron gases on super-fluid helium [1] and in quantum well structures [2], laser cooled ions in traps [3, 4, 5, 6, 7, 8, 9, 10, 11] and most recently dusty plasmas [12]. In Nature, Coulomb crystals are presently expected only to exist in exotic dense astrophysical objects [13].

For infinite OCPs of a single species, the thermodynamic properties are fully characterized by the coupling parameter [14]

$$\Gamma = \frac{1}{4\pi\epsilon_0} \frac{Q^2}{a_{ws} k_B T}, \quad (1)$$

where Q is the charge of the particles, a_{ws} is the Wigner Seitz radius defined from the zero temperature particle density n_0 by $4\pi a_{ws}^3/3 = 1/n_0$. Theoretically, a liquid-solid transition to a body centered cubic (bcc) structure is expected to occur for $\Gamma \sim 170$ [15, 16]. For finite OCPs the situation is more complex. The properties will depend both on the size and shape of the ion plasma, since surface effects cannot be neglected [17, 18, 19, 20, 21].

Ion Coulomb crystals, which for more than a decade have been realized with laser-cooled ion plasmas confined by electromagnetic fields in Penning traps [4, 5, 9] or in radio-frequency (rf) traps [3, 6, 7, 8, 10], offer an excellent opportunity to study finite size effects of OCPs under various conditions. The Coulomb crystal structures studied range from one-dimensional (1D) long cylindrical crystals [3, 6, 7, 8] over 2D thin planar crystals [4] to 3D spheroidal crystals [4, 5, 6, 9]. The 3D spheroidal ion Coulomb crystals reported in Refs. [6, 7] are composed of concentric ion shells formed under the influence of the surface of the Coulomb crystals. Simulations indicate that the ions form a near-2D hexagonal short-range or-

dered structure within each shell [18]. Similarly, shell and short-range order have recently been observed in dusty plasma experiments [12].

Observations of three-dimensional long-range order in Coulomb crystals have previously only been reported in the case of $> 10,000$ laser-cooled ions in a Penning trap [4, 5, 9]. In contrast to Penning traps, in rf traps Coulomb crystals undergo strong quadrupole deformations at the frequency of the applied rf field due to the so-called micro-motion [22] of the ions. Since this motion is known to produce heating [22, 23], it has not been obvious that three-dimensional long-range order could be obtained in rf traps.

In this Letter, we present observations of long-range structure in Coulomb crystals of $^{40}\text{Ca}^+$ ions confined in a linear rf Paul trap. By varying the number of ions in near-spherically symmetric crystals, we have shown that bcc structures indeed can be observed in such traps with the number of ions below a thousand. Furthermore, by varying the density of the ion plasma, experiments have been performed to investigate the dependence of ion plasma structure on the coupling parameter Γ .

The linear Paul trap used in the experiments is described in detail in Ref. [24], so here we give only a brief description of its basic properties. The linear Paul trap consists essentially of four circular electrode rods in a quadrupole configuration. Radial confinement of the ions is obtained by applying a sinusoidally time-varying rf-potential $U_{rf} \cos \Omega_{rf} t$ to diagonally opposite electrodes and the same time varying potential, but with a phase shift of π , to the two remaining electrode rods. Static axial confinement is achieved by having all electrode rods sectioned into three parts with the eight end-pieces kept at a positive dc potential U_{end} with respect to the four center pieces. The electrode rod radius is 2.0 mm, and the closest distance from the trap axis to the electrodes r_0 is 3.5 mm. Each sectioned rod has a 5.4 mm long centerpiece and 20.0 mm long end-pieces. The frequency of the rf field is in all experiments $\Omega_{rf} = 2\pi \times 3.88$ MHz. With the definition given in Ref. [25] of the relevant stability

parameters q and a for the linear Paul trap under the present operation conditions, the geometry of the trap leads to $q = 6.6 \times 10^{-4} U_{\text{rf}} [\text{V}]$ and $a = 5.5 \times 10^{-4} U_{\text{end}} [\text{V}]$. In the experiments the rf-amplitude $U_{\text{rf}} [\text{V}]$ is maximally 500 V, corresponding to $q_{\text{max}} = 0.33$. This value is small enough that in all the experiments a harmonic pseudopotential with rotational symmetry with respect to the trap axis and a uniform zero temperature ion density given by $n_{\text{theo}} = \epsilon_0 U_{\text{rf}}^2 / m r_0^4 \Omega_{\text{rf}}^2 = 1.47 \times 10^3 U_{\text{rf}} [\text{V}]^2 \text{ cm}^{-3}$ can be assumed (ϵ_0 is the vacuum permittivity and m the mass of the ion).

The $^{40}\text{Ca}^+$ ions are produced isotope-selectively by resonance-enhanced photo-ionization of atoms from an effusive beam of naturally abundant calcium [26, 27]. Doppler laser cooling is achieved along the trap center axis by using counter propagating laser beams tuned to the $4S_{1/2}-4P_{1/2}$ transition at 397 nm and with a repumper beam on the $3D_{3/2}-4P_{1/2}$ transition at 866 nm. The radial motion of the ions is cooled indirectly through the Coulomb coupling of the radial and axial degrees of freedom.

Two-dimensional projection images of the positions of the ions in the trap are obtained by detecting the 397 nm light spontaneously emitted during the laser cooling process by a CCD-camera equipped with an image intensifier and a $14\times$ magnification lens system. As indicated in Fig. 1(a), the imaging optic is situated such that the real crystal structure is projected to a plane including the trap axis. Due to the rotational symmetry of the Coulomb crystal boundary around the trap axis, we can deduce from the images their real 3D sizes and hence the number of ions by using the expression for the ion density given above.

With an exposure time of 100 ms used in the experiments, the quadrupole deformations of the Coulomb crystal induced by the rf field are averaged out in the images. The direction of the micro-motion of the individual ions is position dependent as indicated in Fig. 1(a). As a result, only ions close to the horizontal trap plane defined by the horizontal dashed line in Fig. 1(a) and the trap axis, are imaged without micro-motion blurring due to their micro-motion only being in the direction of view (DV) of the camera system.

In Fig. 1(b), an image of a slightly prolate ion Coulomb crystal consisting of about 2300 ions is presented. Clearly visible is a hexagonal structure indicating that the ions, at least close to the central trap plane, must be organized in a well-ordered structure. In order to reveal if the ordered structure persists not only very close to the image plane, in another experiment, the Coulomb crystal was moved down 40 μm by adding a positive dc voltage to the upper two electrode rods as sketched in Fig. 1(c). By doing this one achieves that it is a different part of the crystal that is close to the horizontal trap plane. As seen in the image presented in Fig. 1(d), in this situation we still observe an ordered structure apart from

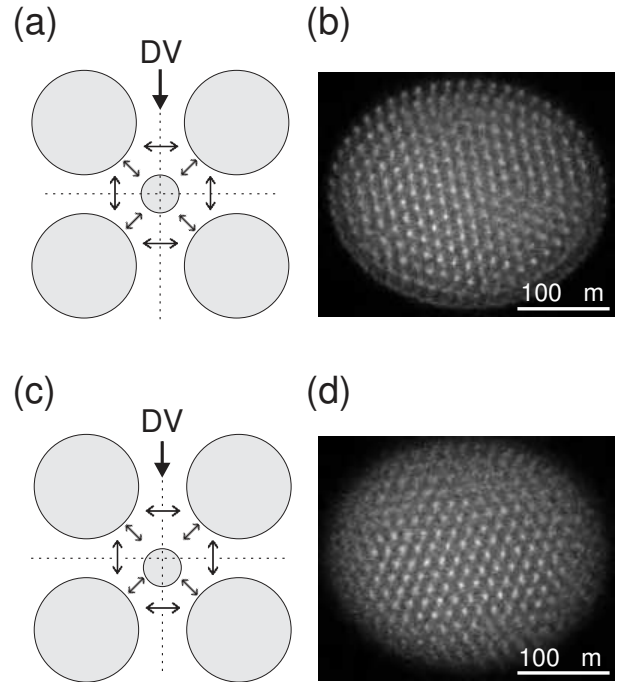


FIG. 1: Observation of hexagonal projections images of a Coulomb crystal consisting of ~ 2300 ions. (a) The four main circles indicate the four cylindrical trap electrode rods viewed along the trap axis. The small circle in the center represents a radially centered Coulomb crystal in the trap. The small double arrows indicate the positional dependent direction of the micro-motion of the ions in the trap. The single arrow denotes the direction of view (DV) for the camera system. The horizontal dashed line indicates the plane including the trap axis in which the direction of micro-motion is along DV. (b) Projection image with the Coulomb crystal radially centered in the trap. (c) Graphical presentation of a crystal vertically displaced. (d) Projection image of a vertically displaced crystal. In both experiments: $U_{\text{rf}}=400$ V and $U_{\text{end}}=15$ V.

at the edges where the fluorescence light originates from ions not being close to the image plane. This experiment substantiates that the ordered pattern observed indeed originates from a three-dimensional long-range ordered structure.

From the pre-knowledge that the ground state of larger ion systems is a bcc configuration [15, 16], it is tempting to assume that the observed structure is indeed a bcc structure observed along the [111] direction. However, also simple cubic (sc) and face centered cubic (fcc) structures will lead to similar hexagonal patterns for the same direction of observation. For a specific side length d of the triangles making up the observed structure, the three cubic structures correspond, however, to different ion densities related by $n_{\text{bcc}} = 2n_{\text{sc}} = 4n_{\text{fcc}}$. The perfect agreement between the expected density of $n_{\text{theo}} = 2.3 \pm 0.2 \times 10^8 \text{ cm}^{-3}$ with the one obtained from the images $n_{\text{bcc}} = 2.1 \pm 0.3 \times 10^8 \text{ cm}^{-3}$ assuming a bcc structure, strongly supports that the observed structure

is indeed a bcc and certainly not a sc or fcc structure. As seen from Fig. 2(a)–(c), the outer shape of the crystal is not critical for observing the long-range structures, at least not as long as the crystal is not too oblate or prolate.

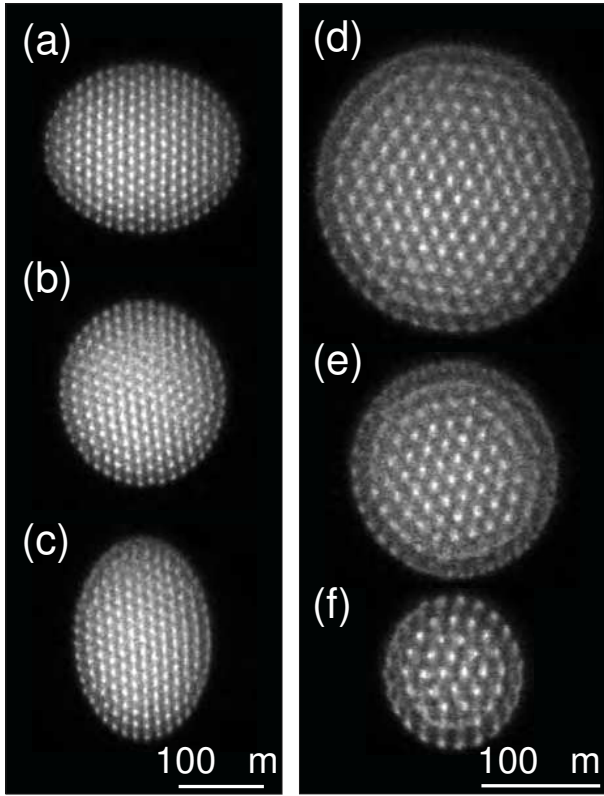


FIG. 2: Projection images of Coulomb crystals. The first column shows three crystal images of the same ensemble of ~ 2000 ion with the trap potentials being $U_{\text{rf}} = 500$ V and (a) $U_{\text{end}} = 27$ V, (b) $U_{\text{end}} = 33$ V, and (c) $U_{\text{end}} = 40$ V, respectively. The second column represents images near-spherical crystals for the same trap potentials $U_{\text{rf}} = 400$ V and $U_{\text{end}} = 21$ V. The number of ions in the crystals is (d) 1700, (e) 770, and (f) 290.

A series of measurements on near spheric crystals with different numbers of ions were done to investigate the size effect of the observation of three-dimensional long-range structures. A few resulting images of this study are presented in Fig. 2(d)–(f). Here, one observes, even in the case of about 770 ions (Fig. 2(e)), very regular structures in the projection images, while in Fig. 2(f) (290 ions) no ordered structures are visible. From MD simulations of ground state configurations of Coulomb crystals, bcc structure has been predicted to be favorable for $\gtrsim 5000$ ions [28, 29]. As will be discussed in detail in a separate publication, there are good reasons to believe that the observed long-range structures are due to the finite thermal temperature [30].

When comparing Fig. 2(d) and (e), it is evident that the relative number of ions in the regular structure de-

creases with the size of the crystals, as may be expected since the outer layer of the crystals is always spheroidal shaped. Another size dependent quantity noticed is the frequency at which ordered structures are indeed observed: The smaller the crystals the more unlikely it is to observe the regular structures. In all cases, since the exposure time of 100 ms is many orders of magnitude larger than both the rf-period and the timescale of crystal vibrations ($\sim 1/\omega_{\text{plasma}}$, with $\omega_{\text{plasma}} \sim 1$ MHz being the plasma frequency), the crystal structures are at least to be considered as metastable states.

To investigate the dependence of the observed long-range order on the coupling parameter Γ , the rf voltage U_{rf} and correspondingly the end-piece voltage U_{end} were varied in a series of experiments such that a ~ 2000 ion Coulomb system stayed spherical, but at different ion densities. In Fig. 3, three projection images for an ion density of (a) $2.3 \times 10^8 \text{ cm}^{-3}$, (b) $1.3 \times 10^8 \text{ cm}^{-3}$, and (c) $0.6 \times 10^8 \text{ cm}^{-3}$ are presented. Unfortunately, it has not been possible to measure the temperature of the ions in the crystals, but MD simulations with 2685 ions in an effective spherical harmonic potential have shown shell structures similar to those presented in Fig. 4(c) when $\Gamma \sim 200$. With this as a reference, Fig. 4(a) and (b) corresponds to $\Gamma \sim 340$ and $\Gamma \sim 280$, respectively. The temperature of the ions must accordingly be ~ 5 mK, which seems reasonable with the Doppler limit being ~ 0.5 mK for $^{40}\text{Ca}^+$. The above inferred values of Γ agree very well with previous MD simulations predicting Coulomb crystallization for a 2000 ion system to appear first when $\Gamma > 250$ [20].

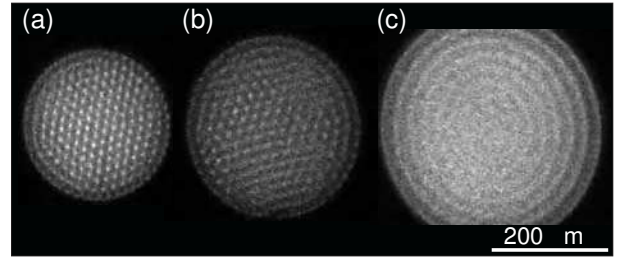


FIG. 3: Projection images of the same ion ensemble in a near-spherical effective trap potential obtained with the trap potentials being (a) $U_{\text{rf}} = 400$ V and $U_{\text{end}} = 21$ V, (b) $U_{\text{rf}} = 300$ V and $U_{\text{end}} = 12$ V, and (c) $U_{\text{rf}} = 200$ V and $U_{\text{end}} = 5.3$ V, respectively.

For crystals with more than ~ 2000 ions, regular projection images are observed, which suggests three-dimensional long-range ordering different from bcc. In Fig. 4, two images of the same ion ensemble ($\sim 13,000$ ions) at two different instants are presented. While the hexagonal structure of Fig. 4(a) and (b) with $d = 17.2 \pm 0.8 \mu\text{m}$ again is compatible with a bcc structure, the rectangular structure observed in Fig. 4(c) and (d) cannot be interpreted as another projection of a bcc structure, but

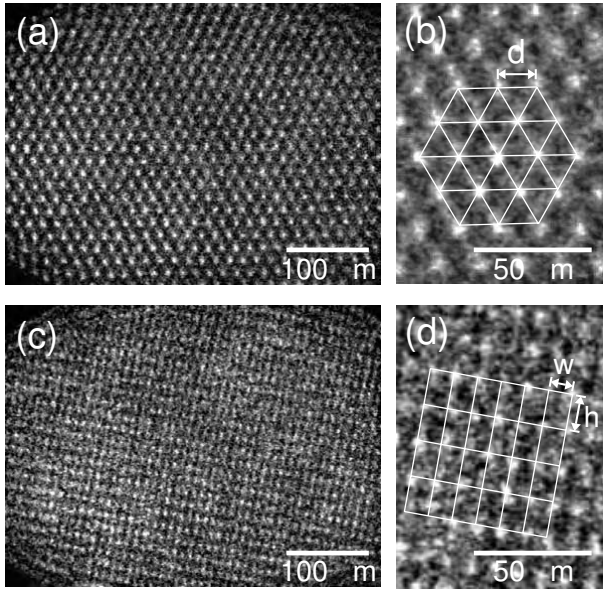


FIG. 4: Projection images of a cold ensemble of $\sim 13,000$ ions. (a) Visible hexagonal structures indicating a three-dimensional bcc structure. (b) Magnification of a section of (a). The side length d is found to be $17.2 \mu\text{m}$. (c) Visible rectangular structure likely indicating a slightly distorted fcc structure. (d) Magnification of a section of (c). Here, $h = 15.2 \pm 0.5 \mu\text{m}$ and $w = 9.71 \pm 0.2 \mu\text{m}$, respectively.

has to relate to another structure. The sides of the rectangle are $h = 15.2 \pm 0.5 \mu\text{m}$ and $w = 9.71 \pm 0.2 \mu\text{m}$, which yields a ratio of the sides of $h/w = 1.55 \pm 0.06$. We do not find that any projection of cubic crystal structures exactly complies with this ratio, but the fcc structure projected in the [211] direction comes close as this has the ratio $h/w = \sqrt{8/3} \simeq 1.63$. For the expected ion density of $n_{\text{theo}} = (2.2 \pm 0.2) \times 10^8 \text{ cm}^{-3}$ the corresponding side lengths of the projected rectangles should for a fcc structure have been $h = 15.2 \pm 0.5 \mu\text{m}$ and $w = 9.3 \pm 0.3 \mu\text{m}$, which does not disagree with the side lengths deduced from the image. The origin of the small discrepancy between the observed and the predicted ratio is at present unknown, but an explanation could probably be found in a micro-motion induced distortion of the fcc lattice. The observation of fcc structures is not so surprising since such structure have already been observed for larger near-spherical Coulomb crystals in Penning traps [5]. Furthermore, MD simulations have as well predicted very small differences in the potential energies of bcc and fcc structures for larger crystals [29].

The reason why the observed bcc or fcc structures always seem to appear oriented in a very specific direction is still not completely understood. However, the non-perfect cylindrical symmetry of the quadrupole trap configuration and the corresponding micro-motion as well as small patch potentials may play a role.

In conclusion, we have shown that despite the fast

micro-motion of ions in Coulomb crystals in linear rf Paul traps, it is indeed possible to obtain three-dimensional long-range ordering. Furthermore, such ordered structures can surprisingly be observed for Coulomb crystals consisting of less than 1000 ions.

We acknowledge financial support from the Carlsberg Foundation as well as from the Danish National Research Foundation: Center for Quantum Optics QUANTOP.

* E-mail: drewsen@phys.au.dk

- [1] C. C. Grimes and G. Adams, *Phys. Rev. Lett.* **42**, 795 (1979).
- [2] E. Y. Andrei, G. Deville, D. C. Glattli, F. I. B. Williams, E. Paris, and B. Etienne, *Phys. Rev. Lett.* **60**, 2765 (1988).
- [3] G. Birkh, S. Kassner, and H. Walther, *Nature* **357**, 310 (1992).
- [4] T. B. Mitchell, J. J. Bollinger, D. H. E. Dubin, X.-P. Huang, W. M. Itano, and R. H. Baughman, *Science* **282**, 1290 (1998).
- [5] W. M. Itano, J. J. Bollinger, J. N. Tan, B. Jelenković, X.-P. Huang, and D. J. Wineland, *Science* **279**, 686 (1998).
- [6] M. Drewsen, C. Brodersen, L. Hornekær, J. S. Hangst, and J. P. Schiffer, *Phys. Rev. Lett.* **81**, 2878 (1998).
- [7] L. Hornekær, N. Kjærgaard, A. M. Thommesen, and M. Drewsen, *Phys. Rev. Lett.* **86**, 1994 (2001).
- [8] T. Schätz, U. Schramm, and D. Habs, *Nature* **412**, 717 (2001).
- [9] J. N. Tan, J. J. Bollinger, B. Jelenkovic, and D. J. Wineland, *Phys. Rev. Lett.* **75**, 4198 (1995).
- [10] N. Kjærgaard and M. Drewsen, *Phys. Rev. Lett.* **91**, 095002 (2003).
- [11] R. Blümel, J. M. Chen, E. Peik, W. Quint, W. Schleich, Y. R. Shen, and H. Walther, *Nature* **334**, 309 (1988).
- [12] O. Arp, D. Block, A. Piel, and A. Melzer, *Phys. Rev. Lett.* **93**, 165004 (2004).
- [13] H. M. van Horn, *Science* **252**, 384 (1991).
- [14] S. Ichimaru, *Rev. Mod. Phys.* **54**, 1017 (1982).
- [15] E. L. Pollock and J. P. Hansen, *Phys. Rev. A* **8**, 3110 (1973).
- [16] W. L. Slattery, G. D. Doolen, and H. E. DeWitt, *Phys. Rev. A* **21**, 2087 (1980).
- [17] A. Rahman and J. P. Schiffer, *Phys. Rev. Lett.* **57**, 1133 (1986).
- [18] R. W. Hasse and J. P. Schiffer, *Ann. Phys.* **203**, 419 (1990).
- [19] J. P. Schiffer, *Phys. Rev. Lett.* **70**, 818 (1993).
- [20] J. P. Schiffer, *Phys. Rev. Lett.* **88**, 205003 (2002).
- [21] D. H. E. Dubin and T. M. O'Neil, *Phys. Rev. Lett.* **60**, 511 (1988).
- [22] R. Blümel, C. Kappler, W. Quint, and H. Walther, *Phys. Rev. A* **40**, 808 (1989).
- [23] J. P. Schiffer, M. Drewsen, J. Hangst, and L. Hornekær, *Proc. Natl. Acad. Sci.* **97**, 10697 (2001).
- [24] M. Drewsen, I. Jensen, J. Lindballe, N. Nissen, R. Martinussen, A. Mortensen, P. Staanum, and D. Voigt, *Int. J. Mass Spectrom.* **229**, 83 (2003).
- [25] M. Drewsen and A. Brøner, *Phys. Rev. A* **62**, 045401 (2000).

- [26] N. Kjærgaard, L. Hornekær, A. Thommesen, Z. Videsen, and M. Drewsen, *Appl. Phys. B* **71**, 207 (2000).
- [27] A. Mortensen, J. J. T. Lindballe, I. S. Jensen, P. Staanum, D. Voigt, and M. Drewsen, *Phys. Rev. A* **69**, 042502 (2004).
- [28] H. Totsuji, T. Kishimoto, C. Totsuji, and K. Tsuruta, *Phys. Rev. Lett.* **88**, 125002 (2002).
- [29] R. W. Hasse, *J. Phys. B* **36**, 1011 (2003).
- [30] M. Drewsen, T. Matthey, A. Mortensen, and J. P. Hansen, submitted manuscript.